Achievable Efficiency and Stability of Supercritical CO$_2$ Compression Systems

Noall, Jeff, S.
Barber Nichols Inc.
Arvada, Colorado 80002, USA
jnoall@barber-nichols.com

Pasch, James, J.
Sandia National Laboratories
Albuquerque, New Mexico, 87185
jjpasch@sandia.gov

The efficiency and stability of supercritical compressors operating near the critical point continue to be topics of interest. Testing of sub-scale power cycles in recent years has indicated compressor efficiency levels lower than expected for full-scale hardware. Such compressor performance levels are consistent with design predictions for these sub-scale systems. Despite this general agreement, there seems to be a persistent perception that supercritical compressors suffer from inherent efficiency and stability disadvantages. The perceived stability issues stem from the well known difficulties associated with operating pumps in two phase conditions (e.g. cavitation phenomena). However, test experience and analysis indicate that full-scale compressor performance near the critical point can be both stable and efficient, even if two phase conditions become present in the compressor flow path. An analysis of the turbomachinery for a representative full-scale power cycle indicates compressor efficiencies significantly higher than that of the sub-scale test data are to be expected.

1   Introduction

In recent years, Sandia National Laboratories has assembled a test loop for a sub-scale supercritical CO$_2$ Brayton power cycle in order to explore the controllability and operability of these cycles. This work, which is part of the DOE GenIV Program, has been described previously [1] [2] [3]. The cycle utilizes two compressors, a main compressor and a recompressor as illustrated in Figure 1. Extensive testing of these compressors has been conducted at both design and off-design conditions. Testing has also been conducted where the compressors have been operated in the two-phase regime in order to assess the stability and durability of the compressor operating under these conditions. The results of these tests have helped to clarify and define performance expectations for the full-scale machines.

2   Test Instrumentation Overview

Pressure and temperature measurement instruments are placed upstream and downstream of the compressor at approximately 28 cm and 40 cm from the compressor inlet and discharge, respectively. Piping ID is 4.29 cm, giving straight run lengths of about 6.5 diameters and 9.3 diameters upstream and downstream of the compression process. Pressure instruments are manufactured by Honeywell, model FPA, P/N 060-F694-02, with a range up to 20.69 MPa and an accuracy of 0.10%, or 20.69 kPa.

Thermocouple instruments are k-type manufactured by Omega, with an accuracy of ± 1.1 °C. Flow rate and density measurement are made with a Micro Motion Coriolis meter, model DH150S154SU. Per the manufacturer, in the conditions tested, the mass flow rate percent accuracy is a function of mass flow rate. An approximate accuracy for the range of conditions tested is $\pm 0.5\%$ of the measured flow rate. Density measurement accuracy is ± 2.00 kg/m^3.
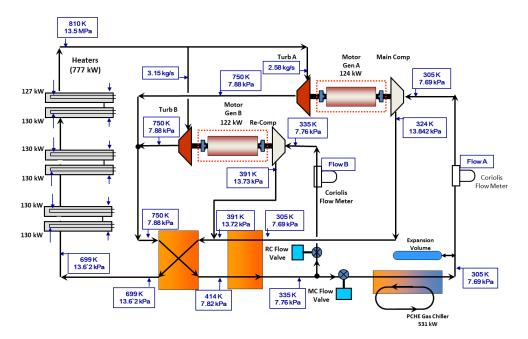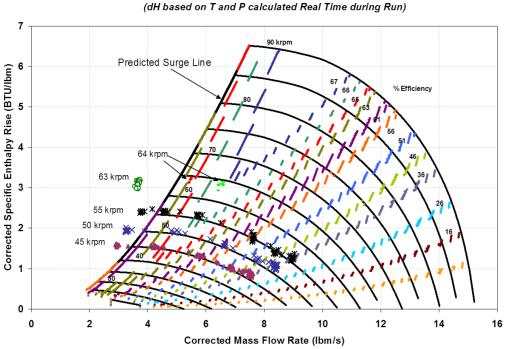
Figure 1: Supercritical CO_2 Brayton Power Cycle Loop.

3   Main Compressor Design Discussion

The main compressor of the Sandia test loop was designed to operate near the critical point where fluid density is high and viscosity comparatively low in order to minimize the compression work required, resulting in a benefit to the overall efficiency of the Brayton cycle. Due to its proximity to the critical point and potential for two-phase operation, the performance of the main compressor is of greater interest. This paper will therefore focus on the performance characteristics of this component.

The main compressor was designed for an inlet pressure and temperature of 7.68 MPa and 305.4 K respectively, producing a discharge pressure of 13.84 MPa at a flow rate of 3.67 kg/s and rotational speed of 75,000 RPM. The overall power level of the thermodynamic cycle was determined by the practical considerations of project funding and limitations on supporting infrastructure. Given the resulting constraints on total heating and heat exchanger capacities, cycle parametric optimizations were conducted in order to maximize the net power output of the cycle. These studies resulted in the cycle shown in Figure 1 with a net cycle power of ≈250 kW. The mass flow rates of both compressors were also a direct result of this study. The main compressor flow rate of 3.67 kg/s in conjunction with a predicted design point efficiency of 66% yields a design power of 55 kW for this component. The determination of the compressor flow rate together with the selection of the shaft speed determines the scale of the compressor.

The speed was limited to 75,000 RPM due to rotordynamic considerations. This results in a non-dimensional specific speed of 0.63, which is less than the optimal value of approximately 0.85 for the given pressure ratio. One would expect higher efficiency if the speed could be increased, however,
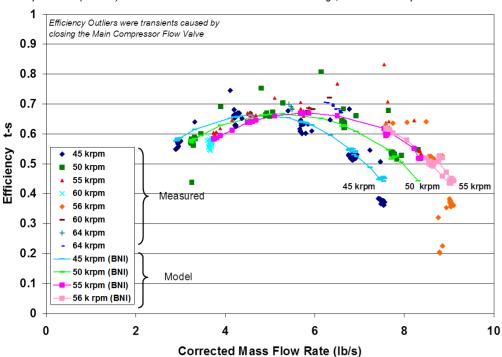
Figure 2: Comparison of test data points to the predicted performance map of the main compressor. Corrected quantities used since inlet pressure and temperature varied during testing. See Reference [4] for definitions.

the benefit would be negated somewhat by the smaller wheel size (and thus larger relative clearances) that would result from a faster design speed. The predicted and observed thermodynamic efficiencies of the main compressor are lower than would be expected from its full-scale counterpart due primarily to clearance effects. In the final design of the turbine-alternator-compressor (TAC) module, the clearance between the impeller exit blade tips and the shroud was 12% of the blade height despite the absolute value of the clearance being held to a very tight value by design standards. A relative blade tip clearance of 12% is very large, and carries with it a substantial performance penalty.

Comparisons between the predicted and tested performance of the main compressor have been given previously by Wright et. al. [2] [3], and are also shown in Figures 2 and 3. Given the difficulty in obtaining precise efficiency estimates from the test data, the tested performance characteristics (efficiency & enthalpy rise) of the main compressor generally agree quite well with design predictions. This implies that the design and prediction tools are correctly capturing performance penalties associated with the small scale of the test hardware. This is important since it implies that the same tool sets can be used to provide meaningful performance predictions of hardware for a full-scale application. One noteworthy difference between the test data and the prediction is in the placement of the compressor surge line. For typical compressor applications, the prediction tool used has been found to place the surge line fairly accurately, though tending to over predict surge margin. For the S-CO$_2$ compressor data, stable operation was obtained at flow rates significantly lower than predicted. This

Main Compressor Measured and Predicted Efficiency
from Spin Test 41 (12/02/08) Based on Motor Power with Corrections for Windage, Friction and Pump Out Vanes

Figure 3: Comparison of main compressor isentropic, adiabatic efficiencies derived from test data vs. predicted efficiency curves.

implies that compression near the critical point, where compressibilities are comparatively low, may benefit from increased surge margin as compared to more typical compressor applications.

4   Full-Scale Compressor Efficiency Estimates

The power cycle shown in Figure 4 shows an example 50 MW S-CO$_2$ plant cycle. The compression requirements for this cycle were used to do sizing and preliminary performance estimates of a full-scale compressor application. In this application, a compressor speed of 15,000 RPM was chosen in order to place the non-dimensional specific speed near optimum with a value of 0.83. This requires a 4.17:1 gearbox ratio assuming a 3600 RPM 50 MWe generator.

The resulting compressor impeller diameter is approximately 225 mm, with a tip speed of about 180 m/s. The low impeller tip speed allows for a wide range of material choices, and freedom to design blade shapes for maximum efficiency. The unique combination of high density and relatively low viscosity of CO$_2$ near the critical point help to keep the viscous losses a smaller fraction of the ideal enthalpy rise produced by the compressor. This will tend to produce a higher compressor efficiency as

compared to operation with more typical working fluids. Although detailed design work of this full-scale compressor has not been completed, preliminary analysis indicates that a compressor isentropic efficiency of 83 to 85% should be realistically achievable.
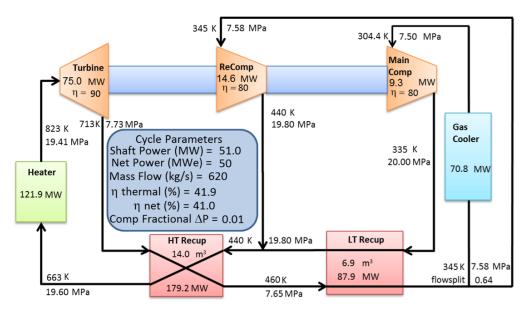

Figure 4: Example 50MW S-CO$_2$ power cycle used to make full-scale compressor performance estimates.

5 Two Phase Compressor Operation

Over the period of the test program to date, the main compressor has accumulated hours of run time in the two phase region within the saturation dome. A subset of this data is plotted in Figure 5, where a plot of the compressor head-flow characteristic is plotted on the left, and a plot showing the saturation dome along with the data points is on the right. In these plots, points that fall within the dome are colored red and points that fall outside of the dome are colored green allowing for easy reference between the two plots. The head and flow coefficients of the compressor are defined by the following relations:

$$\psi = \frac{\Delta h}{U_2^2} \tag{1}$$

$$\phi = \frac{Cm_2}{U_2} \tag{2}$$

where,

$$
\begin{aligned}
\Delta h &= h_{2i} - h_{o1} = \text{isentropic, adiabatic enthalpy rise} \\
U_2 &= \text{impeller tip peripheral speed} \\
Cm_2 &= \text{impeller exit meridional velocity component}
\end{aligned}
$$

In the absence of low Reynold's number effects, data plots of head and flow coefficient for pumps with incompressible media will tend to collapse to a single curve called the pump characteristic, regardless of the operating speed of the pump, or the particular liquid being pumped. For compressors, this is more of an approximation as changes in the gas density which occur through the flow path will tend to introduce offsets to this correlation. The compressor speeds represented in Figure 5 range from 10,000 RPM to 65,000 RPM, with the bulk of the test data taken at a speed of 25,000 RPM.

Since the critical temperature of CO_2 is generally somewhat higher than room temperature, initial fluid conditions in the loop are usually subcritical in both temperature and pressure. Upon start up of the Brayton cycle, the compressor is used as a circulator to push flow through the loop as power is applied to the heaters in order to achieve nominal supercritical conditions. It is thus common for the compressor to encounter two phase conditions at start up, making the ability of the compressor to handle operation within the saturation dome all the more advantageous. It is for this reason that the bulk of the two phase compressor data acquired was at relatively slow "circulation" speeds (typically 25,000 RPM).

For the data presented, the points outside of the dome are represented by the full speed range, but the two phase operation points were limited to speeds less than about 35,000 RPM. The primary objective
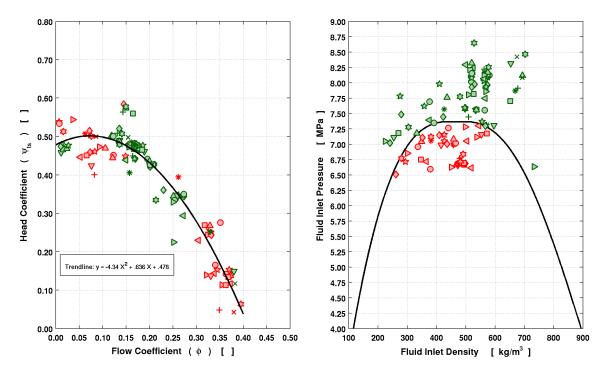

Figure 5: Comparison of compressor performance for points inside and outside of saturation dome.

at the time of start up was not to obtain high speed operation within the dome, but in hind sight, it would have been desirable to run some tests at higher speeds and lower (or no) heat input so that a broader range of operating speeds could be represented in the two phase compressor data. The relatively low speeds associated with the two phase flow are why these data are limited to lower compressor ideal specific enthalpy rises (i.e. pressure rise) as shown in Figure 6.

There are several factors which contribute to the scatter evident in the head-flow characteristic of Figure 5. Note that the calculation of the value of Cm_2 in Eqn. 2 requires a knowledge of the fluid density at the exit of the impeller, which was not directly available from existing instrumentation. Calculations of the flow coefficient thus involved making estimates of the density at this point by assuming a certain percentage of total compressor losses to occur within the impeller itself. This estimation gives rise to additional uncertainty and scatter to the calculations of the flow coefficient. Additionally, the regions of high gradient between density measurements and the corresponding inferred enthalpy level which exist near the top of the saturation dome (vapor side in particular) give rise to added data scatter in the compressor enthalpy rise and hence computed head coefficient.

Given these sources of error, in conjunction with the tendency of compressors to deviate from collapsing to a single non-dimensional form, as mentioned previously, the level of scatter in the head coefficient vs. flow coefficient data is not surprising. More importantly, the amount of scatter in the data corresponding to two phase compressor operation is not noticeably greater than that present in the single phase data. The single phase and two phase data tend to the same characteristic shape, and with comparable levels of data scatter, which implies stable operation of the compressor within the two phase region of the dome. Further, during the two phase operation of the compressor, it was noted that the compressor was operating smoothly with no audible indications of cavitation or other instabilities. Subsequent inspection of the impeller also gave no indication of pitting or other damage to the aluminum blades.

The plots in Figure 6 show time traces of the ideal enthalpy rise as well as the compressor discharge pressure during two phase operation. These time traces indicate smooth, stable operation despite notable changes to the density (quality) during the time period. At first glance, this result is unexpected since some form of cavitation must occur since vapor pockets will grow and shrink or collapse as the two phase fluid interacts with the pressure gradients caused by the impeller blade loading. The key to understanding this phenomena is to realize that the density ratio across the dome in the vicinity of the critical point is quite small compared to that of typical applications.

Consider the saturation states along the 6.75 MPa isobar represented in the data. The saturated density on the liquid and vapor sides of the dome at this pressure are 674.6 kg/m^3 and 272.5 kg/m^3 respectively. These values correspond to a density ratio of only 2.47:1 as compared to density ratios on the order of 1000:1 for many typical pumping applications where cavitation presents a real issue. It is thought that smooth, stable two phase operation of the S-CO$_2$ compressor is possible due to the comparatively very low ratio of saturated liquid and vapor fluid densities. Any liquid-vapor interactions which occur in the impeller must be small enough so as to render the effects benign.
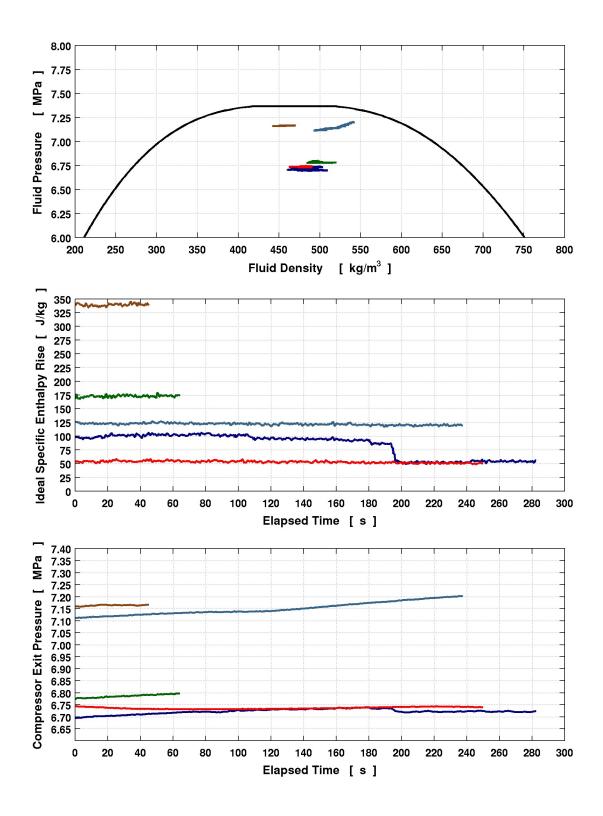
Figure 6: Time traces of compressor discharge pressure and ideal specific enthalpy rise with location within dome.

6 Conclusions

Testing of sub-scale S-CO$_2$ power cycles in recent years has indicated compressor efficiency levels lower than likely would be required to make full scale systems viable. However, the observed low efficiencies are primarily due to the small scale of the test hardware, and are consistent with design predictions for these sub-scale systems. A preliminary performance analysis of a compressor for a full scale 50 MW plant concept indicates that compressor efficiencies in the range of 83% to 85% should be realistically achievable.

A certain amount of attention has been focused on the perceived need to prevent localized two phase flow in the compressor blade passages of S-CO$_2$ applications. Such a view would be well grounded in the context of typical applications. However, test experience has indicated that localized excursions into the saturation dome near the vicinity of the critical point may not present any significant adverse effects.

It is thought that the small ratio of the saturated liquid and vapor densities near the top of the saturation dome are responsible for the benign nature of two phase operation in this region. Prolonged, stable compressor operation has been achieved where inlet conditions were two phase and well within the saturation dome. However, such test experience has been limited to relatively slow speeds as compared to the design speed of the compressor. Further two phase compressor testing should be conducted at higher speeds with correspondingly larger pressure ratios to confirm that such smooth, stable operation will persist under these more general operating conditions.

References

[1] Steven A. Wright, Robert Fuller, Paul S. Pickard and Milton E. Vernon **Initial Status and Test Results from a Supercritical CO$_2$ Brayton Cycle Test Loop**, Proceedings of ICAPP '08 Anaheim, CA USA, June 8-12, 2008, Paper 8266

[2] Steven A. Wright, Paul S. Pickard, Milton E. Vernon, Ross F. Radel and Robert Fuller **Supercritical CO2 Brayton Cycle Power Generation Development Program and Initial Test Results**, Proceedings of the ASME Power 2009 Conference, ASME Power 2009, Albuquerque, New Mexico, July 21-23, 2009.

[3] Steven A. Wright, Paul S. Pickard, Milton E. Vernon and Ross F. Radel **Description and Test Results from a Supercritical CO2 Brayton Cycle Development Program**, 7th International Energy Conversion Engineering Conference August 2-5 2009, Denver, Colorado AIAA 2009-4607

[4] A. J. Glassman, **Turbine Design and Application**, NASA SP-290, pp 58-60.

Acknowledgments